COB-2019-1969

RACING CARS AERODYNAMICS: A NUMERICAL ANALYSIS USING A SIMPLIFIED GEOMETRY

Vinicius Mazetto Leandro
viniciusleandro94@gmail.com
Leonel R Cancino
leonel.cancino@labmci.ufsc.br
Internal Combustion Engines Laboratory - Joinville Technological Center - Federal University of Santa Catarina - LABMCI/CTJ/UFSC.
Rua Dona Francisca 8300, Joinville, SC, Brazil, CEP 89219-600

Abstract. The Formula 1 race car aerodynamics has some basics objectives: the improvement of downforce, focusing on pushing the vehicle down, and the improvement of cornering forces. In this work, a numerical analysis using a simplified geometry of a Formula 1 car was performed. In order to achieve the objective, the test section of a wind tunnel was numerically reproduced and simulated by using computational fluid dynamics. A mesh independence test using four spatial resolution for discretization was performed and the best mesh was used for the numerical analysis, the criteria for mesh choose was a variation on Δc_D less than 2.00%. The simplified geometry was analyzed by surface contributions dividing the same in several components. Three turbulence models (Re-Normalisation Group κ-ϵ model, Standard κ-ω model and Reynolds Stress Model) were used and the numerical responses compared in terms of drag and lift coefficients and component contribution. For all turbulence models used in this work, it was noticed that wheels and wings have a strong effect on drag and lift forces. The values of drag coefficient, c_D, obtained in this work as well as the fluid field around the car are comparable with published data of Formula 1 cars.

Keywords: Racing car aerodynamics, CFD, Lift and drag forces, Turbulence models

1. INTRODUCTION

Aerodynamics is one important aspect along the design process of a car and talking about high-performance racing vehicles, where every second counts for win the race, it is quite the most important aspect. This is easy to see in motor sport categories, as Formula 1, where the vehicle holding the best aerodynamics, has the greater chances of winning the race. Formula 1 vehicles compete with similar vehicles due to competition rules, limiting engine parameters for example. Restrictions arise to limit speed and acceleration, aiming at braking safety and cornering behavior, such as maximum lateral acceleration the rider can withstand. Currently, a Formula 1 vehicle is more like a jet fighter than a ground vehicle. Aerodynamics has become, as previously described, the key to success encouraging teams to invest millions of dollars in this area (Gerhardt *et al.*, 1981). Aerodynamic's designers have three basic concerns: (a) Get a better air friction in order to achieve greater downforce, which will push the vehicle down, minimizing effects from lateral forces at cornering, (b) Minimize aerodynamics drag and turbulence, which have effects against acceleration, reducing vehicle speed and, (c) Automotive design, (Hucho, 1998). After all, Formula 1 is an expensive sport, and no sponsor or spectator wants to see a vehicle with a low-level appearance. Therefore, combining performance and appearance is one of the biggest challenges to the designer. Aerodynamics began to have great influence when it was noticed that there was difficulty to increase the top speed of vehicle, internal combustion engines were then improved as well as other subsystems (Khaled *et al.*, 2012; Diasinos *et al.*, 2015) but, it was not enough to make faster (Hucho, 1998). In the 1960's, competition teams started to use aerodynamic accessories (aids) such as wing and airfoils. Engineers started to notice the similarity of this aids with airplanes wings, and with the aid of Bernoulli's principle, and wing's geometry variations (without flow separation), they were able to impose forces in the vehicle, in order to improve its performance significantly (Hucho, 1998). This papers aims to analyze the numerical response in terms of aerodynamic behavior of a simplified Formula 1 vehicle geometry. Several aspects and properties as pressure, turbulence and velocity field, downforce, drag and recirculation zones of each components and area of the vehicle are then numerically analyzed. Although being simplified, this geometry is useful to better understanding the main technical features of the fluid flow around the vehicle body and the effect of aerodynamic aids. The numerical analysis was performed by using the commercial software ANSYS FLUENT.

2. RACING CAR AERODYNAMICS

Conversely to the case for passenger cars, technical performance is the most important design criteria for racing cars, while for a production car it is important only to have a small aerodynamic drag force, the body of racing cars must create a downward aerodynamic force at the lowest possible drag coefficient. In order to fill this requirement, "add-on" aerodynamic devices are allowed which have to be taken into account during the process of aerodynamic optimization. (Gerhardt *et al.*, 1981; Hucho, 1998)

2.1 Experimental vrs numerical approaches

Thare are two ways to make the aerodynamic analysis of a vehicle, the first is an experimental way by using real scale (prototype) or not (model) geometries in wind tunnels (Kramer *et al.*, 1984). Traditionally, this is the best way to obtain aerodynamic information, however the high cost of tests is usually prohibitive for designers. (Hucho, 1998). Concerning to experimental uncertainties related to wind tunnels, there are several methodologies developed in order to make corrections and of this form get accurate results, (Cooper, 1993; Krajnovic and Davidson, 2005; Cogotti, 2008). The second way arises mainly as an alternative to the high cost of wind tunnel and is the numerical simulation. Also known as CFD (Computational Fluid Dynamics), it consists on the numerical representation of the wind tunnel test section, involving its discretization, where is desired to analyze the fluid flow around the car. Many examples of CFD analysis related to vehicle aerodynamic can be found at literature, some of them involving single or isolated components (Kieffer *et al.*, 2006; Hucho, 1998; Dan Barbut, 2011; Hobeika and Sebben, 2018; Zhang *et al.*, 2018) and other more complete studies involving the full vehicle geometry in the "virtual test section" of the wind tunnel (Mariani *et al.*, 2015; Hanna, 2012; Hucho, 1998; Hassan *et al.*, 2014; Dan Barbut, 2011; Kurec *et al.*, 2019; Cheng *et al.*, 2013; Corin *et al.*, 2008; Altaf *et al.*, 2014; Zhang *et al.*, 2018). CFD provides nice analysis results and the accuracy will be improved as the numerical method (boundary conditions, mesh, turbulence models, etc.) is "well" defined by the CFD expert. Moreover, there are some kind of results that can only be seen on numerical simulation (Hucho, 1998). It is necessary to clarify that CFD and wind tunnel experiments are two complementary methodologies for aerodynamic analysis. CFD requires shorter amount of test time when compared to the wind tunnel, strongly depending on the computational resources (cluster) where the simulation will be done and the spatial resolution of the discretization. The use of CFD as tools for fluid dynamics demand, for many of the engineering applications, the choose and use of a turbulence model. It means that the numerical answer will strongly depend of the selected / choose turbulence model, for vehicular aerodynamics the situation is not different. The chosen turbulence model will strongly imply at the quality and accuracy of the turbulence description of the numerical model and especially in the prediction of surface fluid separation. The fact of vehicles usually hold non-streamlined geometries, the choose of the turbulence model must be done carefully. In order to get realistic values of pressure and velocity fields in most of cases, the choose is done supported on experimental validations in wind tunnels using simplified geometries, (Hucho, 1998).

3. METHODOLOGY

3.1 Simplified vehicle geometry for analyses

The purpose of this paper is to numerically analyze the aerodynamics of a Formula 1 car. However, considering the complexity involved in a simulation by using a plenty-detailed geometry car, a simplified geometry was used to optimize the development of this work, understanding the fluid field around the car and obtaining of this form knowledge about the aerodynamics of this kind of vehicles. Figure 1 shows the simplified geometry. The simplified F1 geometry was obtained from GrabCAD (GrabCAD, 2018). The geometry was developed to represent a simplified Formula 1 vehicle, maintaining its main aerodynamic characteristics such as streamlined design, front and rear wings and underbody. In this way it is possible to capture the fluid dynamic characteristics of the flow field around the vehicle by working with a geometry that requires less computational effort. Table 1 shows the overall dimensions of the car, such as front area used in the numerical analysis.

Table 1. Vehicle main dimensions

Length (mm)	Height (mm)	Width (mm)	Front Area (mm^2)	Height from floor (mm)
4141.38	1055.13	1580.00	101.62	70.00

Concerning to the dimensions fo the computational domain, which refers to the virtual wind tunnel containing the vehicle, in this work was set the length of three vehicles ahead the geometry, five behind and a sufficiently large distance to the side, following the observations and results of works published at literature (Mokhtar *et al.*, 2016; Altinisik *et al.*, 2015; Dube and Damodaran, 2007) so there is no influence of the wall in the flow field, avoiding of this form the obstruction
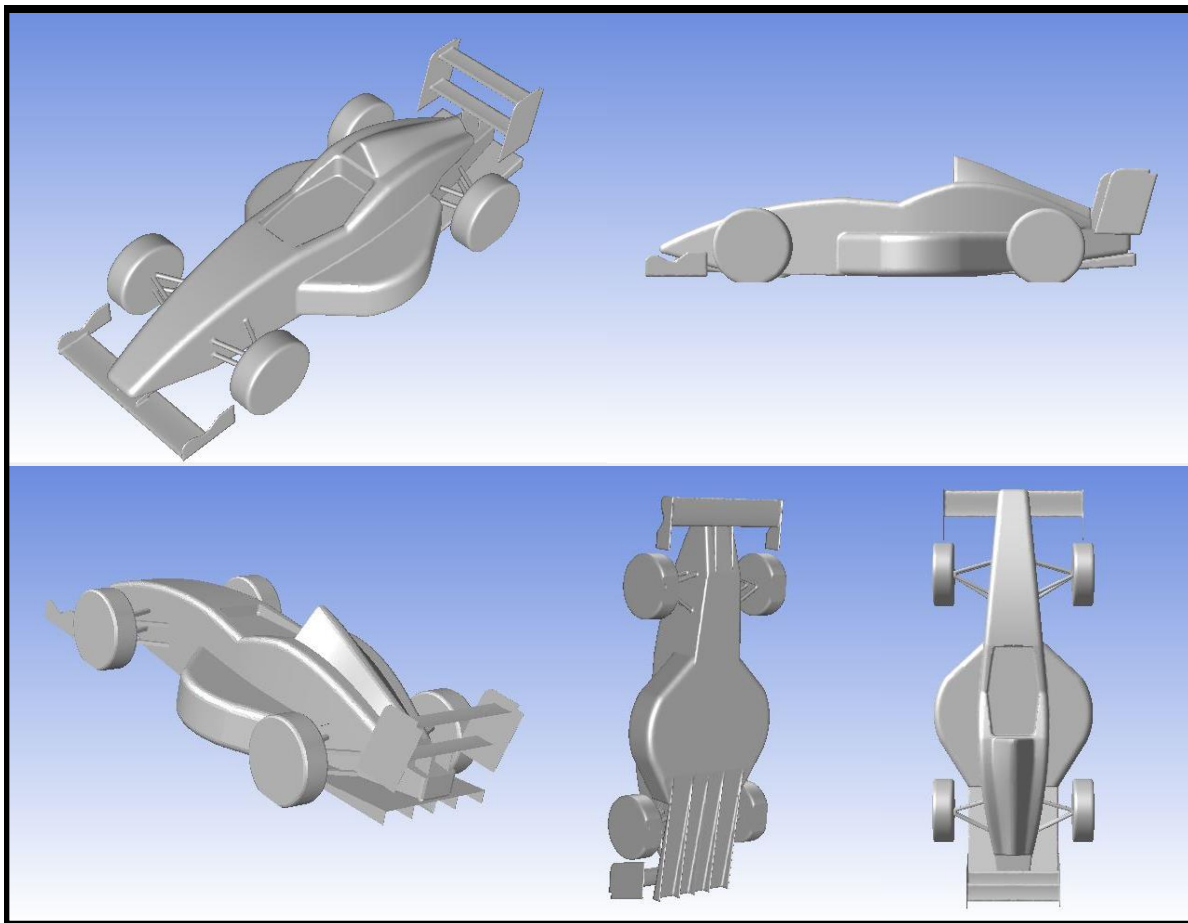
Figure 1. Simplified geometry of the Formula 1 vehicle used in this work

effects. Since the body is symmetrical, only half of the geometry was simulated. Another detail to be noticed is that the base of the wheels and the floor are not collinear. The floor is around 40 mm above the base of the wheels, in order to get a better mesh creation at that region. A Boolean operation must be done to eliminate the geometry of the vehicle and to maintain the wind tunnel.

3.2 Mesh parameters and mesh independence test

Along the mesh generation, some strategies were performed in order to increase the mesh quality. As shown in Figure 2 four control volumes were created: the whole vehicle, the underbody region, the rear and to the nose and cockpit region. The control volumes were created to better describe the interaction of the vehicle surfaces and wind flow, by getting a better mesh because its refinement. The next figure shows the described process.

It is important that the mesh describes as accurately as possible the phenomena occurring in the details along the geometry of the vehicle. Figure 2 shows an overview of the final mesh used in this work. First of all, a mesh with maximum element size of 600 mm was generated throughout the computational domain, with the objective of generating a good enough mesh in the regions with few influence to the results. The type of mesh adopted for the domain was the setup of proximity and curvature, so that there is a standard refinement in regions with curvature and proximity of faces and edges. Refinements were applied in the more critical and important regions for the analysis, where the effects of the flow must be captured more accurately. All the faces of the vehicle and all the control volumes were refined. Mesh independence test was performed by setting four meshes and observing the Δc_D trend along convergence process. Table 2 shows the results of the independence test. Meshes where progressively refined till reach a variation on c_D below that 2.00%.

The final mesh has 8.999.135 elements and 1.543.280 nodes, Table 3 list the final mesh size set-up. To guarantee the quality of the mesh, some statistical aspects were observed as Element Quality, Aspect Ratio and Skewness. The first one evaluates general metric aspects of the mesh quality, having as average of 0.85 (the best possible being equal to 1). The second one checks the aspect ratio of the elements, with an average of 1.7 (the ideal being equal to 1). The third one show how close to the ideal the elements are, having an average of 0.20 (the ideal being equal to 0) for all the four
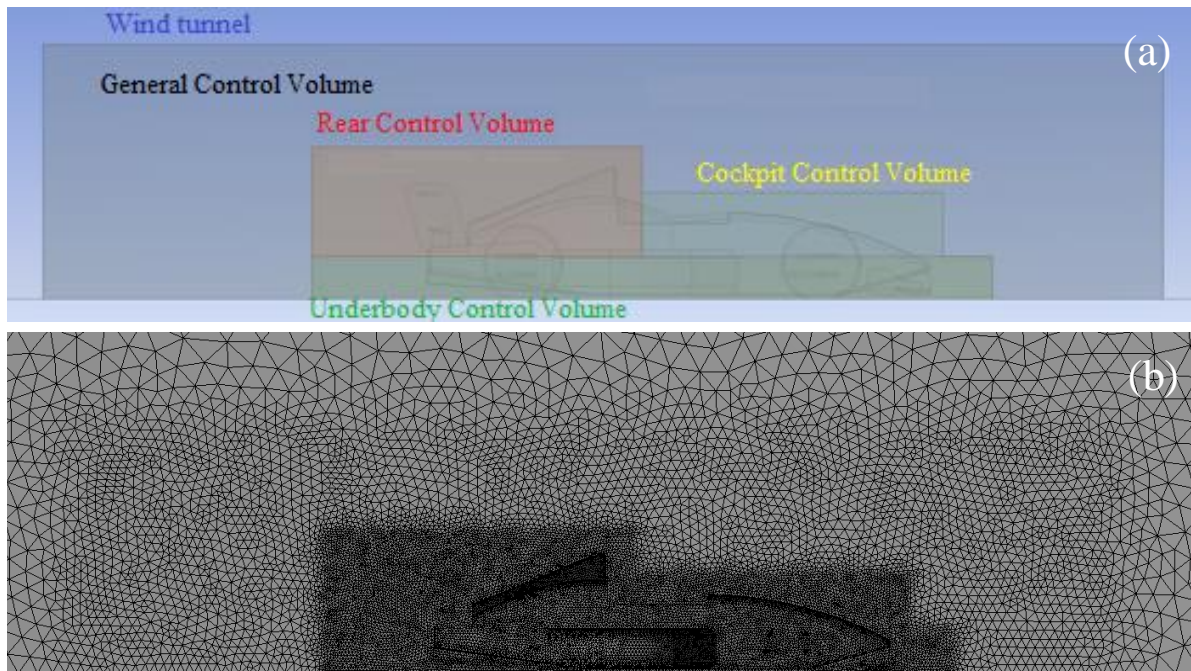
Figure 2. Mesh strategy used for the numerical analysis in this work

Table 2. Mesh independence test

Mesh	Nodes	Elements	Maximum skewness	Elements with maximum skewness	c_D	Δc_D
Mesh #1	331353	1859994	0.9328	85	0.608	—
Mesh #2	554544	3173294	0.9287	62	0.589	3.22%
Mesh #3	859124	4965113	0.9261	43	0.576	2.25%
Mesh #4	1543280	8999135	0.9241	13	0.568	1.40%

meshes. The maximum skewness values for all meshes tested in this work where always below 0.9328, and for mesh #4 the maximum skewness was 0.9241, as shown in Table 2. In this work, the mesh independence test was carried out using the κ-ϵ Re-Normalisation Group (RNG) model, supported by experimental validation of the Ahmed body in previous simulation works (Rocha, 2017) in our research group. For the for the κ-ϵ RNG turbulence model, all the meshes fit the restriction of y+ > 30, the lowest value found in mesh #4 was 270 < y+ < 280. For the Standard κ-ω simulation with mesh #4, the minimum value of y+ found was 260 < y+ < 270. The authors conclude that, for the purpose of this work, the final mesh quality (mesh #4) is satisfactory (ANSYS-FLUENT, 2014).

Table 3. Mesh size set-up used in this work

Vehicle Surfaces (mm)	General control volume (mm)	Other control volumes (mm)
10	60	15

3.3 Simulation set-up

The solver selected was the pressure-based, because it's a analyze of constant density (in-compressible flow). The formulation of velocity used was absolute, disregarding relative velocities outside the system. In this work, three turbulence models were used for numerical predictions. One of the most used models in most cases of CFD at automotive industry is κ-ϵ, providing a good accuracy and robustness, besides having the characteristics to capture very well separations of surface flow, it is ideal for analysis of separation of fluid and surface (ANSYS-FLUENT, 2014). In the model selection, within the κ-ϵ options, the RNG κ-ϵ was selected, which was developed using Re-Normalisation Group (RNG) methods to renormalize the Navier Stokes equations in order of capturing the effects of smaller scales of movement. The RNG model has an additional term in the equation of ϵ that improves the precision of the flow, capturing the effects of swirl in turbulent vortices, generating a better accuracy of drag results. Industrial application of this model shows that it is possible

Table 4. Turbulence models used in this work

κ-ϵ	κ-ω	**Reynolds Stress Model**
Re-Normalization Group	Standard	Linear pressure-strain
	Shear Flow Corrections	Wall BC from κ equation
Non-equilibrium wall functions	Production Limiter	Wall reflection effects
		Non-equilibrium wall functions

to achieve good results in term of values (for example drag coefficient), with precision of 2-5%. Non-equilibrium wall function were used for regions near the walls; because it has better performance in adverse pressure gradients and can cooperate with the separation and connection of the fluid to the surface, which happens constantly in car aerodynamics. The standard κ-ω turbulence models with the shear flow correction and production limiter options was used. In order to compare the numerical results with a model without the Boussinesq hypothesis (eddy viscosity assumption), the Reynolds Stress Model with wall reflection effects and non-equilibrium wall function options was also used. Table 4 summarizes all the turbulence models used in this work.

Table 5 shows the boundary conditions used in this work for all runs. The value of 56 m/s is equal to the vehicle moving at 200 km/h, a value slightly below the average working rate of a Formula 1 vehicle that constantly reaches 300 km/h. It was no chosen to use a higher velocity value to not reach a subsonic regime, which is equivalent to approximately 0.3 Mach number. It is worth noting that in this simulation the movement of the wheels were considered in order to capture a better phenomenology of the flow, where the vehicle has stationary walls and the wheels non-stationary walls. For external flow, ANSYS-FLUENT advises a turbulence intensity for velocity inlet of 1% and 5% pressure outlet. Other values needed to be provided for the aerodynamics calculations as frontal area and air density.

Table 5. Boundary conditions

F1 Vehicle	Wheels	Interior	Outlet	Inlet Velocity
Stationary wall / Viscous Forces	89.6 rad/s	Air flow	Pressure outlet	56 m/s
			Turbulence intensity 5%	Turbulence intensity 1%
			Turbulent viscosity rate = 10	

A strategy was designed to better execute the numerical model. The simulation was divided into two steps, the first (100 iterations) will be a first order spatial discretization, which makes the solution easier to start without compromising the simulation at the beginning. Later, the simulation was continued to be performed with a more complex second-order spatial discretization until the results converge at the order below of 1.0×10^{-3}.

4. Results and discussion

4.1 Total pressure and pressure coefficient

Figure 3 shows the total pressure and pressure coefficient (c_P) field in the vehicle body. Note that all figures have the same scale on pressure and c_P, (-2900 < pascal < 2300 and -3.15 < c_p < 1.02), of this form it is easy to see the differences of valued predicted by the three turbulence models used in this work. The influence of each region on the flow, such as high pressure on the front wing and certain points of the rear wing, is clear in order to increase vehicle downforce and increase pressure in low pressure unwanted drag. In the same image, it is evident the regions of decoupling of the flow (low pressure zones), having as a large percentage of influence the region just behind the cockpit. The images on the left is possible to analyze the pressure coefficient along the vehicle, being able to observe the zones of high and low pressure, as well as points of stagnation and acceleration of the flow. In function of high flow velocities at the underbody region reach a negative pressure coefficient of c_p = -2.07 for κ-ϵ, c_p = -3.12 for κ-ω and c_p = -3.04 for RSM. That low values of c_p are common to be found in real Formula 1 vehicles, (Hucho, 1998). The observed span in the pressure coefficient (downforce) for all turbulence model returns that there is a similar variation on total pressure predicted by the turbulence models, this is noticeable in the right side of Figure 3 and in absolute values of total pressure the data post processing shows p = -1849 pascal for κ-ϵ, p = -2193 pascal for κ-ω and p = -2846 pascal for RSM.

4.2 Velocity fields and pathlines

Figure 4 shows the velocity field at vehicle surface (left) and path lines colored by velocity magnitude (right). In the left side, because the non-slip condition, only velocity contours are seen at wheels, because rotational moving wall was used as boundary condition. In the data post processing is possible to see the low speed zones in front of the vehicle, in
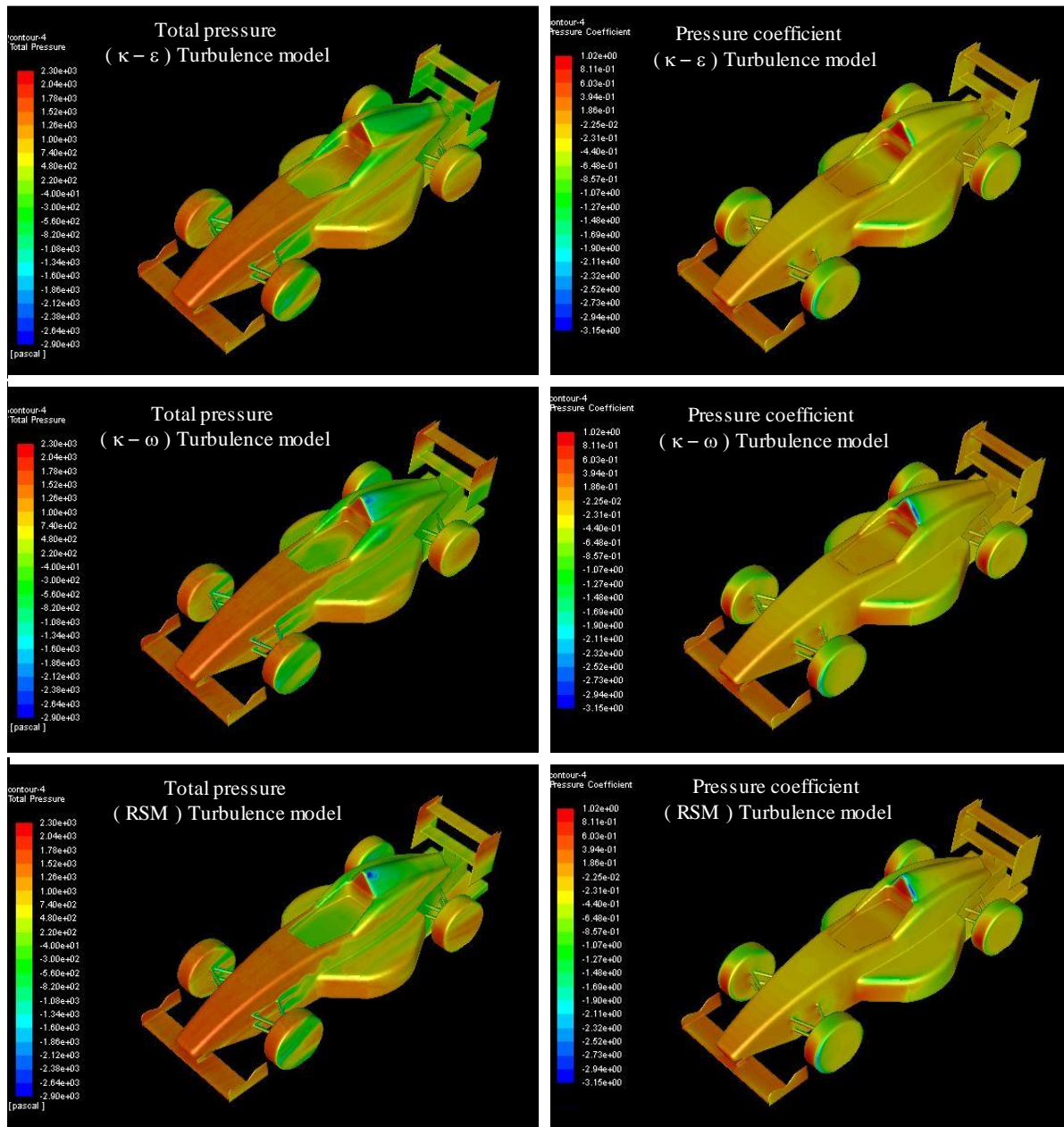
Figure 3. Total pressure (left), Pressure coefficient (right)

the cockpit region and in the rear of the vehicle where surface fluid detachment occurs, in blue. There are also zones of fluid acceleration in red as in the region of obstruction of the flow below the front wing and in the region of the nozzle near the cockpit. A plane was created on the outer surface of the wheel and on it is possible to see the behavior of the fluid due to rotation. In the front wheel, it is possible to check the region where the longitudinal vortices (just behind the wheel) is formed which has caused a great impact on the drag of the vehicle, (see Figure 5).

In Figure 5 was opted for visualization by path lines, in order to be able to see clearly the trajectory of the particles along the flow and to verify the formation of the vortex. With the previous images is evident the influence on the drag of the region just behind the cockpit and the wheels, because of this, plans were created to analyze the vortex formed in these regions. In this figure, on the left, is possible to verify the longitudinal vortex formed due to the movement of the wheel, which has high turbulent kinetic energy contributing to the drag. However, it should be remembered that the wheel movement generates the jetting effect, which presses the air out of the stagnation zone forcing an amount of air to the back of the wheels, generating an increase in pressure and consequently contributing to the drag decrease. In the same figure, now on the right, it is clear the high influence of drag in the rear region of the vehicle, where there is vortices formation shortly after the cockpit due to change of geometry. Note that, it is possible to make quite the same observations for all
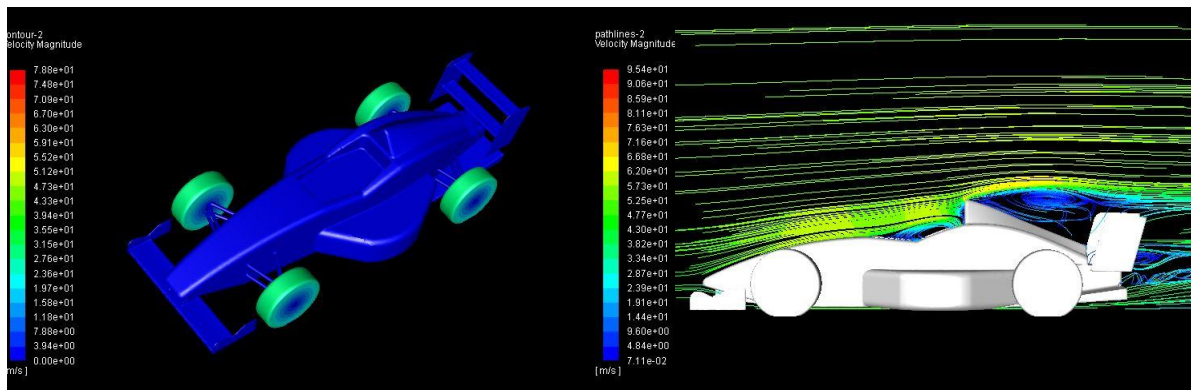
Figure 4. Non-slip condition (left), Recirculation zones and flow separation zones - path lines colored by velocity magnitude (right)

Table 6. Drag and lift coefficients

Component	κ-ϵ				κ-ω				RSM			
	c_D	c_D (%)	c_L	c_L (%)	c_D	c_D (%)	c_L	c_L (%)	c_D	c_D (%)	c_L	c_L (%)
F1 Vehicle	0.304	53.73%	-0.126	22.19%	0.287	51.89%	-0.041	7.03%	0.278	53.18%	-0.112	17.87%
Rear Wheel	0.103	18.14%	0.060	—	0.091	16.38%	0.074	—	0.086	16.45%	0.080	—
Front Wheel	0.115	20.33%	0.097	—	0.114	20.57%	0.103	—	0.110	21.00%	0.097	—
Rear Wing	0.011	2.02%	-0.059	10.37%	0.028	5.09%	-0.166	28.41%	0.018	3.54%	-0.117	18.72%
Front Wing	0.013	2.22%	-0.273	47.97%	0.015	2.70%	-0.278	47.55%	0.012	2.35%	-0.290	46.38%
Underbody	0.020	3.56%	-0.111	19.47%	0.019	3.37%	-0.099	17.01%	0.018	3.47%	-0.107	17.03%
Total	0.566	100%	-0.412	100%	0.553	100%	-0.407	100%	0.522	100%	-0.448	100%

the turbulence models tested in this work. There are small differences on the figures the right side of Figure 5, however, at left side the κ-ω turbulence model shows a very well defined vortex in the upper rear part of the car. That vortex modified completely the pressure field in the car surface having an strong impact in the predicted values of drag and lift, as observed in Table 6.

4.3 Turbulence intensity and turbulent dissipation rate

Still analyzing the longitudinal vortex formed, in Figure 6 the formation of the same can be analyzed throughout the geometry of the vehicle, which have high turbulent intensity, generating a downward flow between them (inducing a peak of negative pressure) which has the largest contribution to the total drag of the vehicle. this can be observed for all the turbulence model tested in this work. The higher values of turbulence intensity, I, are observed for the κ-ω turbulence model ($I = 29\%$), followed by the RSM turbulence model ($I = 27\%$)and the lowest one was for the κ-ϵ turbulence model ($I = 22\%$). Small differences were observed in the turbulent dissipation rate (ϵ). In Figure 6 it can observed that wheels pursues the higher values of turbulence intensity (I) and turbulent dissipation rate ϵ, in agreement with the high values of aerodynamic drag representing zones of high fluid separation.

4.4 Drag and lift coefficients - global and component contributions

In order to verify the actual influence of aerodynamic aids on the vehicle, it was set up in the vehicle simulation to analyze the data separately from each part of the vehicle, front wing, rear wing, underbody and wheels. In this way, drag and lift data can be obtained for each of the previously mentioned parts and for the vehicle as a whole. Table 6 list the results for all the turbulence model used in this work. It is possible to observe the great influence that the spinning wheels have on the vehicle drag, especially the front wheel due to its vortices of high turbulent intensity shown in the figures above. It was also possible to prove the effectiveness of the use of aerodynamic appendages, even contributing to the increase of the drag, they were very efficient in the downforce increase, representing about 70% of the negative lift (downforce) coefficient and also for the reduction of drag in the rear of the vehicle due to the rear wing and the underbody. As shown in Table 6, different turbulence model returns different values of aerodynamic coefficients, however, all of them are close to the value of $0.5 < c_p \; 0.6$, what is reasonable for a simplified Formula 1 vehicle geometry.
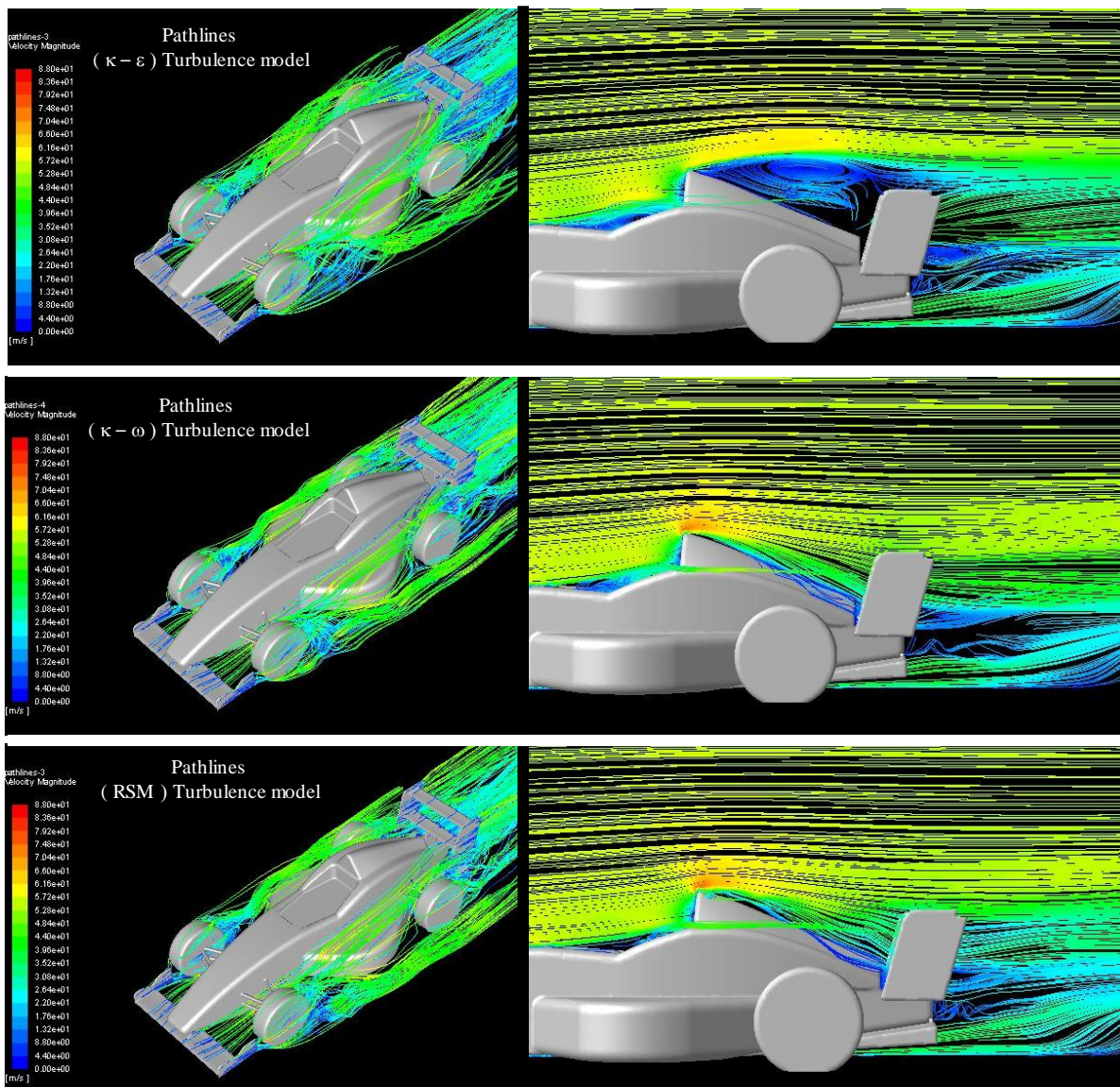
Figure 5. Path lines colored by velocity magnitude at several locations and views

5. CONCLUSSION

Fluid simulations in the automotive industry are of great importance, providing good results with a much lower cost and time when compared to the real test, such as a wind tunnel for vehicular aerodynamics. Know how to develop a good mesh, to make the most of the available computational effort, and knowing how to apply the correct boundary conditions related to fluid mechanics as well as turbulence models will return satisfactory results. The present work allowed the use of techniques in the area of computational fluid dynamics, in order to better understand the application and analysis of fluids in computational environment. The obtained results where satisfactory, resulting in analyses of velocity field, pressure field, vortex analysis data, drag and lift information of the vehicle available to the reader. It can be clearly seen how aerodynamic appendages influence this type of vehicle and how the design of the vehicle generate a desired increase in downforce. The value obtained from c_D was satisfactory, considering all simplification of the geometry and that the actual c_D of a Formula 1 vehicle is around 0.7 to 1.10, according to the study made by the Université de Liége (Dimitriadis, 2018) on aerodynamic experimental data, depending on the circuit. This range of drag coefficient can be confirmed by aerodynamic study of a vehicle of Formula 1 made by Ravelli and Savini (2018), where the c_D of the full vehicle is 1.16. Comparing with this study, it is known that c_D depends directly on the frontal area of the vehicle and the drag force acting on it. If the drag force is fixed, and a linear comparison of the c_D with the frontal areas of the vehicles is made (having a difference of 21% between the two geometries), it is possible to obtain a c_D of 0.959, which fits within the c_D range shown earlier. The simplifications of the geometry lie mainly in the design of the vehicle, at the angles of
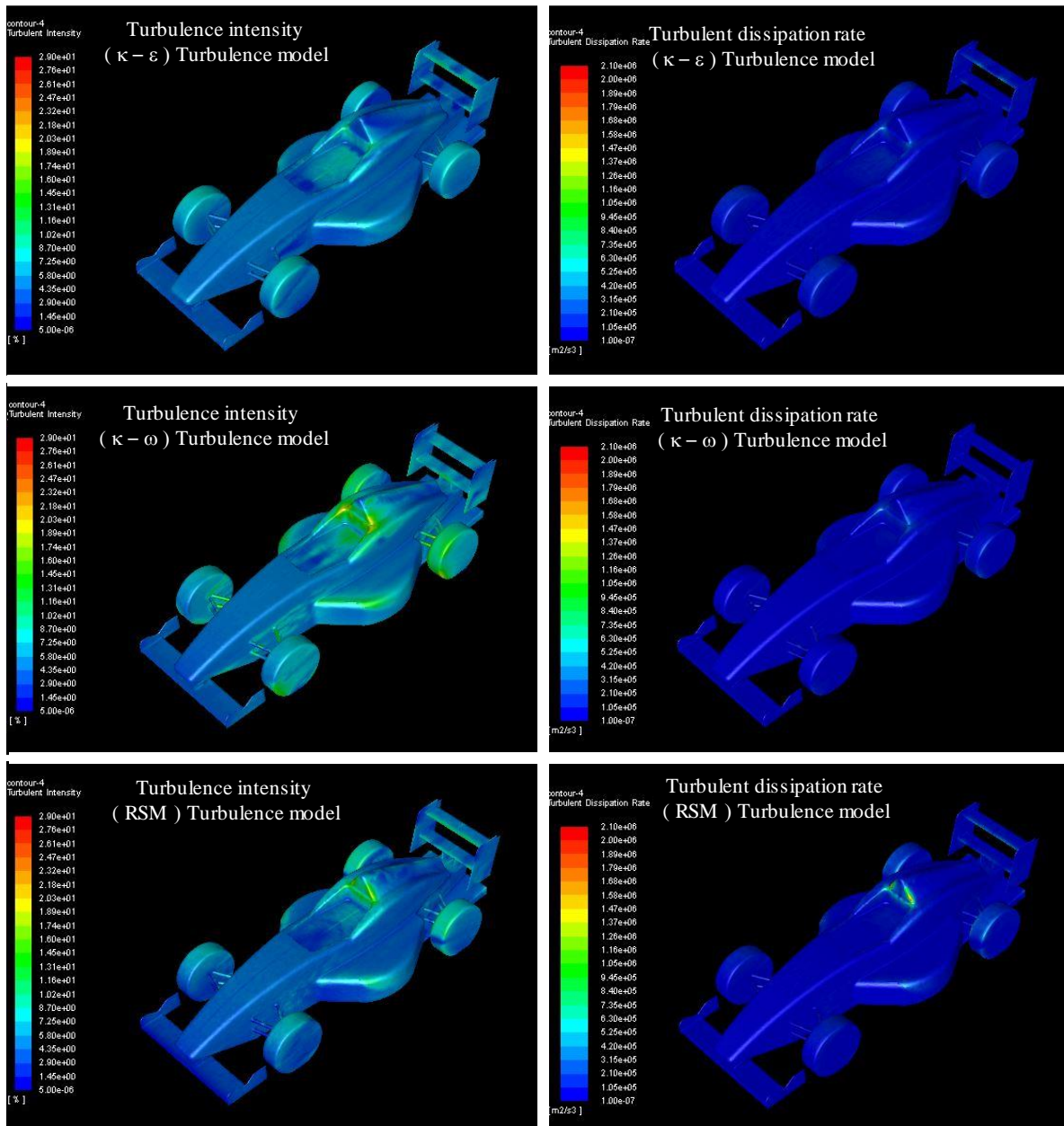
Figure 6. Turbulence intensity (*I*) (left) and Turbulent dissipation rate (*ε*) (right)

the wings of the aerodynamic appendages and in the side-pod region, which is closed and does not allow an interaction of the internal and external flow.

6. ACKNOWLEDGEMENTS

7. REFERENCES

Altaf, A., Omar, A.A. and Asrar, W., 2014. "Passive drag reduction of square back road vehicles". *Journal of Wind Engineering and Industrial Aerodynamics*, Vol. 134, pp. 30 – 43. ISSN 0167-6105. doi:https://doi.org/10.1016/j.jweia.2014.08.006.

Altinisik, A., Kutukceken, E. and Umur, H., 2015. "Experimental and Numerical Aerodynamic Analysis of a Passenger

Car: Influence of the Blockage Ratio on Drag Coefficient". *Journal of Fluids Engineering*, Vol. 137, No. 8. ISSN 0098-2202. doi:10.1115/1.4030183. URL `https://doi.org/10.1115/1.4030183`.

ANSYS-FLUENT, 2014. "Ansys fluent lecture 7: Turbulence modeling - introduction to ansys fluent 15.0 release". ANSYS Confidential.

Cheng, S., Tsubokura, M., Okada, Y., Nouzawa, T., Nakashima, T. and Doh, D., 2013. "Aerodynamic stability of road vehicles in dynamic pitching motion". *Journal of Wind Engineering and Industrial Aerodynamics*, Vol. 122, pp. 146 – 156. ISSN 0167-6105. doi:https://doi.org/10.1016/j.jweia.2013.06.010. The Seventh International Colloquium on Bluff Body Aerodynamics and Applications (BBAA7).

Cogotti, A., 2008. "Evolution of performance of an automotive wind tunnel". *Journal of Wind Engineering and Industrial Aerodynamics*, Vol. 96, No. 6, pp. 667 – 700. ISSN 0167-6105. doi:https://doi.org/10.1016/j.jweia.2007.06.007. URL `http://www.sciencedirect.com/science/article/pii/S0167610507001249`. 5th International Colloquium on Bluff Body Aerodynamics and Applications.

Cooper, K., 1993. "Bluff-body aerodynamics as applied to vehicles". *Journal of Wind Engineering and Industrial Aerodynamics*, Vol. 49, No. 1, pp. 1 – 21. ISSN 0167-6105. doi:https://doi.org/10.1016/0167-6105(93)90003-7.

Corin, R., He, L. and Dominy, R., 2008. "A cfd investigation into the transient aerodynamic forces on overtaking road vehicle models". *Journal of Wind Engineering and Industrial Aerodynamics*, Vol. 96, No. 8, pp. 1390 – 1411. ISSN 0167-6105. doi:https://doi.org/10.1016/j.jweia.2008.03.006.

Dan Barbut, E.M.N., 2011. "Numerical study on aerodynamic drag reduction of racing cars". *INCAS BULLETIN*, Vol. 3, p. 15 âĂŞ 22. ISSN 2066 âĂŞ 8201. doi:https://doi.org/10.13111/2066-8201.2011.3.3.2. INCAS BULLETIN.

Diasinos, S., Barber, T.J. and Doig, G., 2015. "The effects of simplifications on isolated wheel aerodynamics". *Journal of Wind Engineering and Industrial Aerodynamics*, Vol. 146, pp. 90 – 101. ISSN 0167-6105. doi:https://doi.org/10.1016/j.jweia.2015.08.004. URL `http://www.sciencedirect.com/science/article/pii/S0167610515001968`.

Dimitriadis, G., 2018. "Vehicle aerodynamics - lecture 4: Fast cars". `http://www.ltas-aea.ulg.ac.be/cms/uploads/VehicleAerodynamics04.pdf`. Accessed: 2018-09-01.

Dube, P. and Damodaran, V., 2007. "Numerical Approach to Determine Wind Tunnel Blockage Correction for the External Aerodynamics of a Vehicle". *14th Asia Pacific Automotive Engineering Conference, Hollywood, California, USA*, Vol. 2007-01-3462. URL `https://www.sae.org/publications/technical-papers/content/2007-01-3462/`.

Gerhardt, H., Kramer, C., AmmerschlÃd'ger, T. and Fuhrmann, R., 1981. "Aerodynamic optimization of a group-5 racing car". *Journal of Wind Engineering and Industrial Aerodynamics*, Vol. 9, No. 1, pp. 155 – 165. ISSN 0167-6105. doi:https://doi.org/10.1016/0167-6105(81)90086-6.

GrabCAD, 2018. "Grabcad community". `https://grabcad.com/`. Accessed: 2018-08-01.

Hanna, R.K., 2012. "Cfd in sport - a retrospective; 1992 - 2012". *Procedia Engineering*, Vol. 34, pp. 622 – 627. ISSN 1877-7058. doi:https://doi.org/10.1016/j.proeng.2012.04.106. URL `http://www.sciencedirect.com/science/article/pii/S1877705812017195`. ENGINEERING OF SPORT CONFERENCE 2012.

Hassan, S.R., Islam, T., Ali, M. and Islam, M.Q., 2014. "Numerical study on aerodynamic drag reduction of racing cars". *Procedia Engineering*, Vol. 90, pp. 308 – 313. ISSN 1877-7058. doi:https://doi.org/10.1016/j.proeng.2014.11.854. URL `http://www.sciencedirect.com/science/article/pii/S1877705814029919`. 10th International Conference on Mechanical Engineering, ICME 2013.

Hobeika, T. and Sebben, S., 2018. "Cfd investigation on wheel rotation modelling". *Journal of Wind Engineering and Industrial Aerodynamics*, Vol. 174, pp. 241 – 251. ISSN 0167-6105. doi:https://doi.org/10.1016/j.jweia.2018.01.005.

Hucho, W.H., 1998. *Aerodynamics of Road Vehicles: From Fluid Mechanics to Vehicle Engineering*. SAE, 4th edition.

Khaled, M., Hage, H.E., Harambat, F. and Peerhossaini, H., 2012. "Some innovative concepts for car drag reduction: A parametric analysis of aerodynamic forces on a simplified body". *Journal of Wind Engineering and Industrial Aerodynamics*, Vol. 107-108, pp. 36 – 47. ISSN 0167-6105. doi:https://doi.org/10.1016/j.jweia.2012.03.019. URL `http://www.sciencedirect.com/science/article/pii/S0167610512000761`.

Kieffer, W., Moujaes, S. and Armbya, N., 2006. "Cfd study of section characteristics of formula mazda race car wings". *Mathematical and Computer Modelling*, Vol. 43, No. 11, pp. 1275 – 1287. ISSN 0895-7177. doi:https://doi.org/10.1016/j.mcm.2005.03.011. URL `http://www.sciencedirect.com/science/article/pii/S0895717705004590`.

Krajnovic, S. and Davidson, L., 2005. "Influence of floor motions in wind tunnels on the aerodynamics of road vehicles". *Journal of Wind Engineering and Industrial Aerodynamics*, Vol. 93, No. 9, pp. 677 – 696. ISSN 0167-6105. doi:https://doi.org/10.1016/j.jweia.2005.05.002. URL `http://www.sciencedirect.com/science/article/pii/S0167610505000450`.

Kramer, C., Gerhardt, H. and Regenscheit, B., 1984. "Wind tunnels for industrial aerodynamics". *Journal of Wind Engineering and Industrial Aerodynamics*, Vol. 16, No. 2, pp. 225 – 264. ISSN 0167-6105. doi:https://doi.org/10.1016/0167-6105(84)90009-6.

Kurec, K., Remer, M., Mayer, T., Tudruj, S. and Piechna, J., 2019. "Flow control for a car-mounted rear wing". *International Journal of Mechanical Sciences*, Vol. 152, pp. 384 – 399. ISSN 0020-7403. doi:https://doi.org/10.1016/j.

ijmecsci.2018.12.034. URL `http://www.sciencedirect.com/science/article/pii/S0020740318318484`.

Mariani, F., Poggiani, C., Risi, F. and Scappaticci, L., 2015. "Formula-sae racing car: Experimental and numerical analysis of the external aerodynamics". *Energy Procedia*, Vol. 81, pp. 1013 – 1029. ISSN 1876-6102. doi: https://doi.org/10.1016/j.egypro.2015.12.111. URL `http://www.sciencedirect.com/science/article/pii/S1876610215027605`. 69th Conference of the Italian Thermal Engineering Association, ATI 2014.

Mokhtar, W., Madagi, C. and Hasan, M., 2016. "Further study of wall interference for high blockage vehicles in closed test section wind tunnels". *International Journal Of Modern Engineering Research (IJMER)*, Vol. 6, No. 10, pp. 58 – 70. ISSN 2249-6645. URL `http://www.ijmer.com/papers/Vol6_Issue10/Version-2/H61025870.pdf`.

Ravelli, U. and Savini, M., 2018. "Aerodynamic simulation of a 2017 f1 car with open-source cfd code". *Journal of Traffic and Transportation Engineering*, Vol. 6, pp. 155 – 163. doi:10.17265/2328-2142/2018.04.001.

Rocha, S.L., 2017. "Análise numérica do campo de escoamento externo na geometria de referência ahmed para aplicações automotivas". Undergraduate thesis, Federal University of Santa Catarina, Automotive Engineering <https://repositorio.ufsc.br/handle/123456789/181918>.

Zhang, C., Uddin, M., Robinson, A.C. and Foster, L., 2018. "Full vehicle cfd investigations on the influence of front-end configuration on radiator performance and cooling drag". *Applied Thermal Engineering*, Vol. 130, pp. 1328 – 1340. ISSN 1359-4311. doi:https://doi.org/10.1016/j.applthermaleng.2017.11.086.

8. RESPONSIBILITY NOTICE

The author(s) is (are) the only responsible for the printed material included in this paper.